Multi-LED Multi-Datastream Dome Bulb for Dense Visible Light Communication Networks

Sajad Saghaye-Polkoo
CREOL
University of Central Florida
Orlando, FL, USA
sajad.saghaie@knights.ucf.edu

Pooya Nabavi
Electrical & Computer Eng.
University of Central Florida
Orlando, FL, USA
pooya.nabavi@knights.ucf.edu

Murat Yuksel
Electrical & Computer Eng.
University of Central Florida
Orlando, FL, USA
murat.yuksel@ucf.edu

Kyle Renshaw
CREOL
University of Central Florida
Orlando, FL, USA
krenshaw@creol.ucf.edu

ABSTRACT

In this paper, we consider multi-datastream VLC networks serving dense IoT deployments and propose a "dome bulb" that consists of a multi-LED array with a dome-shaped lens structure to separate each LED's beam for spatial reuse. Each LED has Lambertian irradiance distribution that can be collected and directed to receiver location using a wide field-of-view (FOV) lens system. Within the FOV, each LED's divergence angle is narrowed to improve spatial reuse, which also brings the problem of spotty lighting. We analyze the dome bulb in terms of illumination uniformity and Signal-to-Interference-Noise Ratio (SINR) provided to receivers in the room. We also present a channel model based on the simulated SINR.

CCS CONCEPTS

• Networks • Network types • Wireless access networks • Wireless local area networks

KEYWORDS

Visible Light Communications, Illumination Uniformity, Multi-Datastream optical communication networks.

ACM Reference format:

Sajad Saghaye-Polkoo, Pooya Nabavi, Murat Yuksel, and Kyle Renshaw. 2020. Multi-LED Multi-Datastream Dome Bulb for Dense Visible Light Communication Networks. In *Proceedings of ACM MOBICOM'20. ACM, New York, NY, USA, 6 pages.*

1 Introduction

The number of wireless devices surpassed the wired ones on the Internet. The Internet-of-things (IoT) is becoming a reality as more devices are connecting to the Internet. The IoT era is imposing dense deployment of devices in small areas. Supporting thousands of IoT devices in a dense setting will be challenging via legacy radio frequency (RF)-based network access. The wireless spectrum is becoming scarcer and yet necessary for the IoT devices and applications to progress and become further integrated into the society. One option to solving the spectrum scarcity problem is to deploy ultra-small access points. As the size of the access point decreases, spatial reuse increases, and it becomes possible to use the same spectral bands for accommodating more devices. However, it is questionable if this approach will be economically feasible. Keeping the cost of deploying more access points under control will be the key challenge of this approach. An alternative, as well as a complementary approach, is to use emerging higher frequency bands, such as millimeter-wave (mmWave) or optical wireless, to complement the RF-based wireless access networks. As a special form of optical wireless networks, Visible Light Communication (VLC) offers a niche complementary solution to the spectrum scarcity in indoor settings. Since it does not interfere with legacy RF bands, it can work as a complement. Further, since Light Emitting Diodes (LEDs) are becoming the mainstream lighting method, VLC mashes well with the increasing trend of LED-based solid-state lighting.

Most of the VLC research considered single-datastream approaches utilizing diffuse optics or multi-input multi-output (MIMO) techniques, e.g., multiple LEDs as transmitters and multiple photodetectors (PDs) as the receiver. The Typical approach has been to increase the divergence angle of the LED beams to obtain uniform lighting and transmit one datastream to a single receiver. Even though the receiver might have multiple PDs, they are used to receive a single datastream. Due to the wide-angle LED beams, these techniques do not take advantage of spatial reuse of the VLC bands.

In this paper, we consider multi-datastream VLC networks serving dense IoT deployments and propose a "dome bulb" that consists of a multi-LED array with a dome-shaped lens structure to separate each LED's beam for spatial reuse. Each LED irradiance can be collected by a fast lens and be steered to a certain angle to improve spatial reuse, which also brings the problem of spotty lighting. We analyze the dome bulb in terms of illumination uniformity, Signal-to-Noise Ratio (SNR), and Signal-to-Interference-plus-Noise Ratio (SINR) provided to receivers in the room. Our main contributions include:

LIOT'20, September 21, 2020, London, United Kingdom

ACM ISBN 978-1-4503-8099-7/20/09...$15.00
https://doi.org/10.1145/3412449.3412550

- A multi-LED dome-shaped bulb design that allows multiple VLC downlinks for settings where dense deployment of receivers is the norm.
- A thorough study of irradiance maps for the multi-LED bulb system while varying defocus amount.
- Analysis of the tradeoff between SINR and lighting uniformity in the dome bulb.
- Characterization of the VLC channel being offered by the dome bulb.

The rest of the paper is organized as follows: First, we survey the literature on multi-LED VLC systems and position our work. Then, in Section 3, we present the dome bulb concept and give a detailed description of a particular design. Section 4 presents results from ZEMAX simulation of the bulb system, and studies the channel being offered by it. Finally, we conclude in Section 5.

2 Related Work

One way to taxonomize the VLC systems is to consider the number datastreams simultaneously accommodable by the system. Single-datastream VLC uses the VLC channel for transmitting data to only one receiver, while multi-datastream VLC can serve multiple receivers in the same room at the same time. A significant amount of the VLC literature focused on single-datastream solutions that can offer great lighting uniformity, typically via diffuse optics.

Recently, there have been studies [1,2] exploring the potential for multi-datastream VLC solutions while tackling new problems they bring. For instance, to reduce the crosstalk between the multiple datastreams, narrow-angle LED beams are used in such VLC systems and this causes spotty lighting. Further, the problem of associating or assigning LEDs to individual receivers in the room needs to be solved on the fly. Hence, along with their great potential, the multi-datastream VLC systems bring new optimization problems, some of which have been successfully solved [3,10,11]. Further, integration of such multi-datastream VLC designs with the existing WiFi access networks has recently been explored as well. The VLC-WiFi integration brings new challenges in user-to-access point association [12], proper handling of uplink and downlink separately [13], and differentiated treatment of omni-directional WiFi channels and directional VLC channels [14].

Placing multiple lighting structures has received notable attention. Attocells [4] have been considered to exploit spatial reuse of VLC channels in a single room. Each LED-based bulb is considered as an atto-cell and serves as an access point. However, this approach works in large rooms and does not address the case when IoT devices are deployed denser than the bulbs. For IoT applications involving tens or hundreds of wireless devices in a small room, the only option, with atto-cells, is to perform time-sharing of the VLC channel from few bulbs/attocells that could be fixtured in that room. Hence, solutions are needed for dense VLC networks where the number of bulbs deployable in a room is not sufficient to provide access to many IoT devices simultaneously.

Designing bulb structures for multi-datastream VLC has received attention as well. Placing LEDs at different locations on the ceiling of the room [5,9], tessellating a hemispherical shape with many LEDs [3], and increasing transmit or receive diversity by placing multiple LEDs or PDs conformally [6,7] were explored. We propose a new bulb structure where LEDs are placed at the back of a dome-shaped lens system.

3 Dome Bulb

Desired goals of a dense VLC system include (i) the capability to send multiple transmissions from the same lighting fixture, (ii) minimize the crosstalk between these simultaneous transmissions, and (iii) attain uniform lighting across the room. The first two goals are achievable by our recent work on imaging-based beam steering (IBBS) for free-space optical (FSO) communication [8]. In IBSS, an array of individually addressable emitters placed at the focal plane of a lens system. The geometric positions of emitters on the object plane determine the direction of steered light in the horizontal and the vertical axes. This technique enables a very low divergence beam and beam shaping control as well as multiplex communication using separate datastreams for each emitter in the array. However, this design does not consider the lighting uniformity. In relation to the third goal for dense VLC systems, there is an inherent tradeoff between the lighting uniformity and SINR. In our dome bulb for VLC, we consider the defocus parameter which tunes the placement of the LED array with respect to the focal point of the lens system. We next give detailed description of a dome bulb design, which we later use for simulations in the paper.

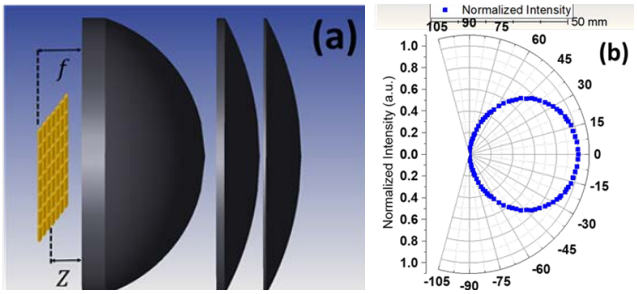

Figure 1. (a) Design of dome bulb consists of an array of individually addressable LEDs close to the focal plane of a lens system. (b) Lambertian distribution of the power of one LED.

The design of the dome bulb based on IBBS system for VLC is shown in Figure 1(a). Three commercially available uncoated lenses with the focal distance of $f_1 = 75\ mm, f_2 = f_3 = 150\ mm$ and identical diameter of 75 mm combined to make an equivalent imaging system with an effective focal length of 44.8mm (back focal length ~$10\ mm$). The working F# and image space F# are ~0.9 to collect the high emission cone of 41.7° (total FOV~83°) from the source. The optical system is designed to illuminate room area of ~$4\ m^2$ at the distance of 2 m from the last lens surface with a total magnification of M≈49. The transmitter (Tx) plane made of an array of 7×7 of individually addressable emitters consists of commercially available $5 \times 5\ mm^2$ phosphorus white LED with the flux intensity of 610 to 710 lm (GW P9LT32.EM-PTPU-XX51-1) separated by 1 mm in x and y directions. To be consistent, we

consider 610 lm for each LED through the simulations. The source position at distance Z from the first surface which may not be exactly the back focal plane of the imaging system. We could modulate each LED up to 25 MHz with an open eye-diagram. Figure 1(b) shows the angular irradiance distribution of an LED that indicates a Lambertian distribution which can be collect up to ~60% by the lens. Although the size of our transmitter is fairly small ($7 \times 10 \times 10\ mm^3$), it can illuminate the fair large area for a demo and proof of concept application since illumination of a larger area is possible with adjustment in source and lens sizes.

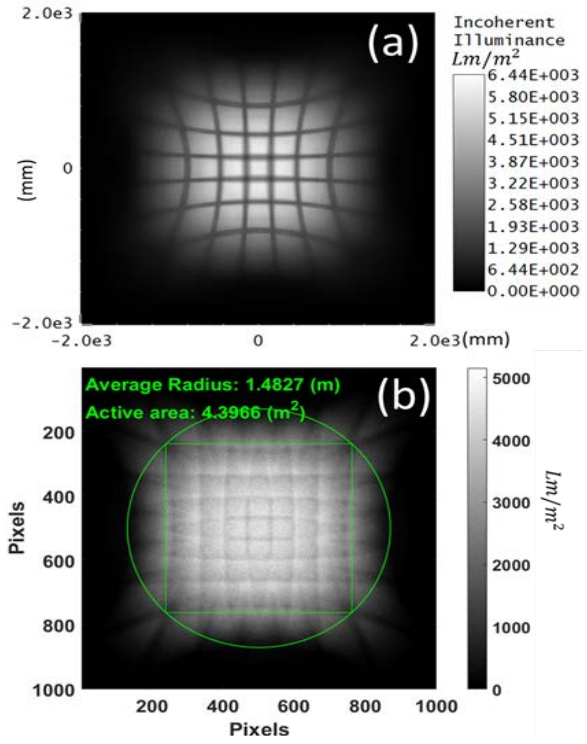

Figure 2. (a) Irradiance map of dome bulb at the distance of 2 m from the last lens surface when emitters are close to the focal plane. (b) The same pattern as (a) while 15.6% defocus is applied. Inset square shows the active illumination area and circle shows boundary separating dark and illuminated areas.

4 Simulation Results

In order to evaluate the dome bulb design, we consider SINR for a user in the room and uniformity of lighting in the room. We quantify the uniformity as the ratio of standard deviation to average (i.e., coefficient of variation) of the light intensity across the room floor. We vary the defocus parameter Z and observe how SINR and the uniformity change. Based on our dome bulb system, we first calculate irradiance maps on the room floor using ZEMAX simulations and then calculate SNR and SINR.

4.1 Irradiance Maps

We first look at the irradiance maps from our bulb system. We observe how the irradiance maps change by varying the defocus parameter Z. Figure 2(a) shows the image plane (room area) normalized irradiance map produced by non-sequential ray tracing in ZEMAX for 10^7 rays from each emitter in the 7x7 array. The floor is divided by 1,000x1,000 pixels for a 4x4 m^2 room size. As expected, when the source is at the back focal plane its image is resolved in an image plane and vertical and horizontal dark lines, resembling the spacing between emitters. This indicates an effective spatial optical filtering functionality of the lens system. However, this may not be desirable for uniform room illumination.

Positioning the LED array at Z = 3 mm far from the first surface (Figure 1(a)) produces 15.6% defocus and covers dark areas (which are the lines the illumination areas of LED emitters) by overlapping the boundary of illumination area of each emitter. This is shown as an intensity map in Figure 2(b). Proper setup of the defocus is vital to avoid discontinuity in the data stream for a mobile receiver (Rx) in the illuminated area. In Figure 2(b), the circle is showing the criteria of illumination. The circle radius is chosen to be the average distance of all pixels that their luminous flux falls between 25% to 35% of maximum luminous flux in the map centered at the center of the map. This provides a good estimation for the active (useful) illumination area shown by a square inside the circle for data streaming. The size of the active area is 4.4 m^2 in our design. Within this active area, we measured normalized intensity and observed 0.15 standard deviation with the mean value of 0.65, which shows the uniformity is in an acceptable range. As shown in Figure 2(b), a smaller square can be used to achieve higher uniformity at the cost of reduction of the active illumination area.

4.2 SNR and SINR Maps

Understanding the communication efficiency from the dome bulb involves calculating SINR for an IoT device downloading from an LED at the bulb. To quantify how good the downlink from the bulb is, we consider an IoT receiver located on the floor and assign the LED that corresponds to the location of the receiver as the main transmitter (Tx). In a dense VLC network, there will be other IoT devices located in other locations on the floor. So, we assume that beams from the other LEDs are interference.

To investigate SINR, we calculate the power received by from the main Tx at the photo-detector attached to the IoT device, and compare it to all the other interfering signals produced by other emitters. We assume a detector with $8 \times 8\ mm^2$ $(2 \times 2\ pixels)$ aperture area. We place this Rx in different locations in the active area ($524 \times 524\ pixels$) randomly for 50,000 times. At any location, the LED that delivers the highest power to the Rx is considered as the main Tx and sum of the power from all other LEDs received by Rx considered as interference. We perform this simulation for different defocus, Z, values. The result for 15.6% defocus is shown in Figure 3. Comparison between Figure 3(a), which shows only the signal, and Figure 3(b), which shows only the interference, reveals that the central area receives more interference than the main signal. This effect can be seen in the SINR map shown in Figure 3(c). One remedy for this problem could be tuning of the central LEDs (i.e., the ones located at the center of the LED array) with a different power or when a central LED is used as a Tx, its neighbor emitters is used just for

illumination, not for data transmission. The latter can be considered as a time division multiplexing approach, which may also be inevitable when there are more than one IoT devices falling into the illumination area of the same LED.

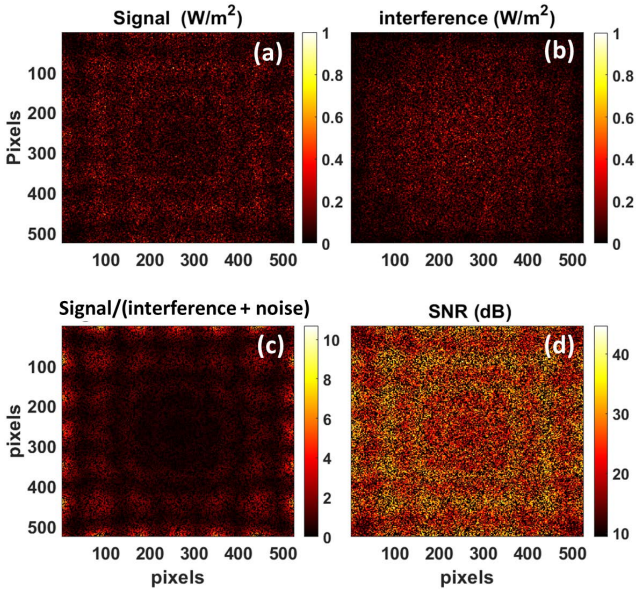

Figure 3. 15.6% defocus: (a) Normalized signal received by Rx from the main Tx for 50K different detector locations in the active area. (b) Normalized interference received by Rx from all other emitters except the main Tx. (c) SINR map of the room active area. (d) SNR map of the room active area.

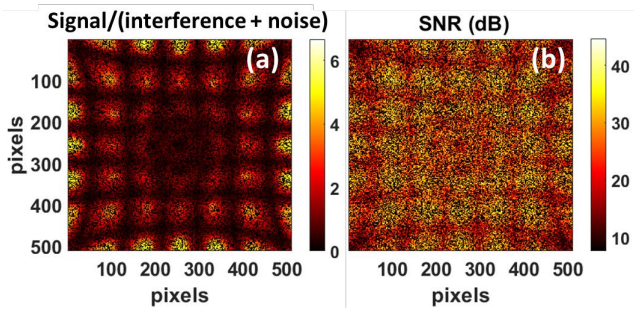

Figure 4. 11.1% defocus: (a) SINR and (b) SNR maps of the room active area.

Observing signal-to-noise ratio (SNR) at the IoT receiver allows us to see how much interference (or crosstalk) affects the reception quality. Figure 3(d) shows SNR of the active area, defined by P_{sig}/P_{noise}, where P_{sig} is the power of the signal extracted from Figure 3(a) and P_{nois}, is the sum of shot noise and thermal noise. Thermal noise, $k_b T \Delta f$, calculated at room temperature (300 Kelvin) with value of 5.15×10^{-15}, where k_b is the Boltzmann Constant. The shot noise is calculated based on current, $i_{noise} = \sqrt{2qI_{total}\,\Delta f}$, received by Rx from all emitters where q is the electron charge, I_{total} is calculated from noise and signal power maps in Figure 3(a),(b) , and Δf =12.5 MHz is the half bandwidth of our Tx. We consider a silicon detector with a responsivity of 0.35 A/W at 550 nm for simplicity. For 15.6% defocus the minimum value of SNR is ~45 dB and, unlike SINR, the central area does not have noticeably lower SNR. This verifies that crosstalk between the LED beams is the main issue for attaining high throughput.

Reducing defocus sharpens the dark areas between the illumination areas of LEDs. Figure 4 shows SINR and SNR maps for 11.1% defocus. While just 4.5% closer to the full focus, the spatial filtering of the optical system is more pronounced and the active area slightly shrinks to $4.17m^2$.

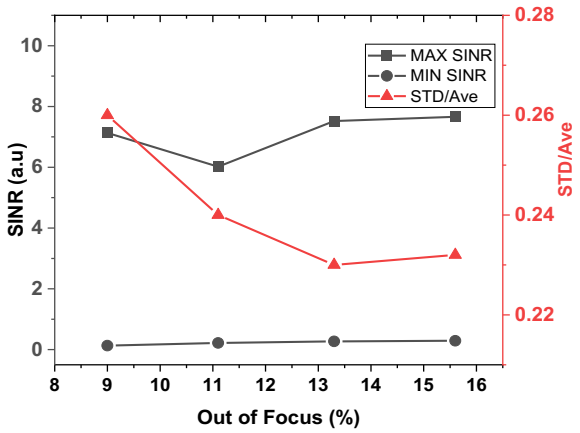

Figure 5. The left Y-axis shows SINR and the right Y-axis shows the ratio of the standard deviation to average of room active area irradiance map.

We now use the SINR and SNR maps to find the sweet spot for defocus. Figure 5 shows minimum, maximum of SINR, and ratio of standard deviation to the average (STD/Ave) of the room active area for different defocus values. This ratio is a measure of uniformity of light intensity distribution on the floor, and the smaller value is more desirable. While the minimum SINR increases slightly with an increase in defocus, the change in the maximum of SINR is noticeable. Our results showed that, with increase of the defocus, the maximum of SINR does not change significantly and its trend is not linear. It is not surprising that uniformity measure, STD/Ave of SINR, is high at lower defocus, but its minimum is close to 13.3% defocus which is corresponding to Z = 4 mm in Figure 1(a). This suggests that the higher defocus may not necessarily translate to higher uniformity and this parameter should be optimized separately for different optical systems. These results show that there is a need to optimize the defocus amount for attaining a balance between better uniformity (i.e., more defocus) and higher throughput (i.e., higher SINR), which is left for future work.

4.3 Estimated Channel Behavior

A key capability of the ZEMAX simulation is that it allows us to observe how the VLC downlink channel of our dome bulb will be. In particular, using the SINR maps, we empirically plot the histogram of SINR for a receiver randomly located at the active

area in the room. The histogram of the SINR at the receiver plane is demonstrated in Figure 6(a) for 15.6% and Figure 6(b) for 11.1% defocuses. As shown in both cases, the Birnbaum-Saunders distribution can effectively predict the statistical behavior of SINR. Lower defocus results in a larger spread and fatter tail in the SINR distribution. This means more blind spots in terms of reception quality but more spots with high reception quality as well. For a mobile IoT receiver, this will translate to an intermittent channel as it moves around within the active area of the room.

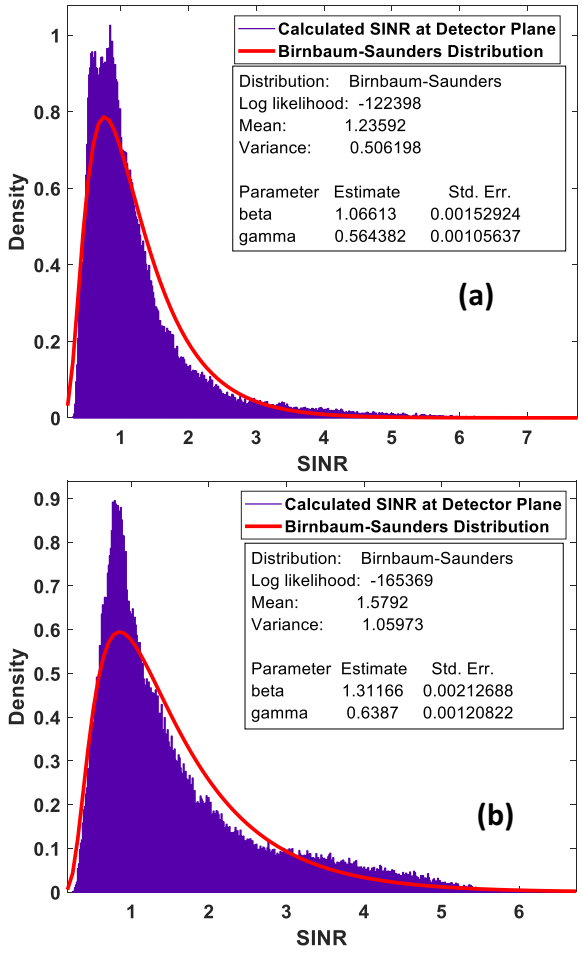

Figure 6. Histogram and estimated distribution for SINR when defocusing is set to (a) 15.6% and (b) 11.1%.

In order to observe the behavior of the SINR distribution in its tail, we look at the probability-probability plots. Figure 7 depicts the Normal probability plots corresponding to our SINR at out of focus percentages of 15.6 % and 11.1%. Using these Normal probability plots we can compare the empirical distribution function of SINR with specified theoretical distribution functions, which is Birnbaum Saunders in this case (based on Figure 6). Furthermore, the Normal probability plot magnifies the small and high probability samples, which helps us better see the empirical distribution's tails. As shown in Figure 7, the Birnbaum Saunders probability density function is one of the most appropriate candidates with the highest goodness of fit to statistically model the SINR in the various cases of out of focus percentages. As shown in Figure 7(b), decreasing the defocusing increases the probability of achieving higher SINR but in the expense of having less illuminance uniformity in the environment.

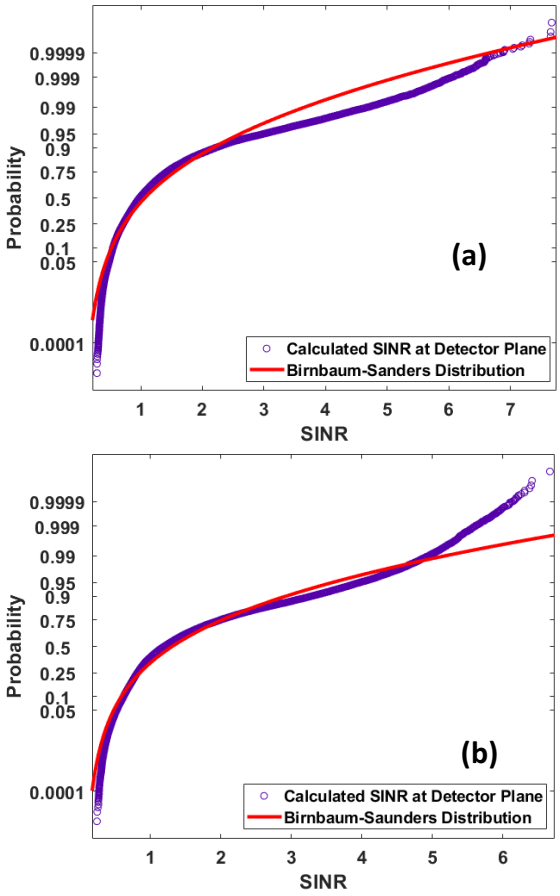

Figure 7. Normal Probability plot of the SINR when defocusing is set to (a) 15.6% and (b) 11.1%.

When SNR is considered, the best fitting distribution changes. Figure 8 demonstrates the Normal probability plot of SNR. As shown in Figure 8(a) and (b), the Generalized Pareto distribution can predict the statistical behavior of the SNR with better fit than Birnbaum-Saunders when defocusing is set to 15.6 % and 11.1% and no interference is present, respectively. This shows that optical interference caused by multiple data-carrying optical beams can effectively change and shift the statistical behavior of SINR from Birnbaum-Saunders in the case of maximum interference (Figure 7) towards generalized Pareto distribution in the case of no interference (i.e., Figure 8).

6 Summary and Future Work

We presented a dome bulb system for dense VLC networks. The bulb system offers multi data-stream capability where an array of LEDs simultaneously transmit data to receivers. We conducted a

set of simulations to investigate the statistical behavior of the illumination uniformity, SINR, and SNR being offered by the dome bulb. Using ZEMAX Optical Studio, we simulated the light beams exiting from the bulb through ray-tracing of the data-carrying beams towards a detector randomly located in the room, and observed the overall achieved illumination factor due to the concurrent emission from LEDs with Lambertian power distribution. We obtained irradiance maps over the room floor, which enabled us to define a practical area of larger than $4\ m^2$ for data-steaming and illumination simultaneously with a compact model. Using a real-time simulation, we showed how SINR and illumination uniformity interacts with each other in the indoor environment. Our results showed that using an optical system enables spatial filtering which leads to high SINR.

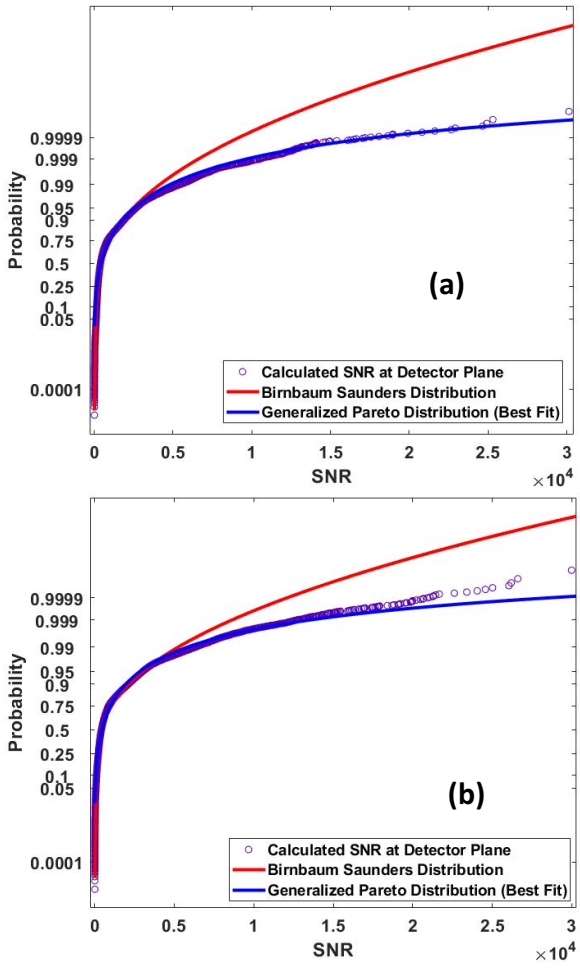

Figure 8. Normal Probability plot of the SNR when defocusing is set to (a) 15.6% (b) 11.1%

We considered different defocusing scenarios to study the trade-off between SINR and luminance uniformity at the room floor. The results for the dome bulb system are promising in that it is possible to attain decent active area in a room by using a compact lens system in front of an LED array. In particular, we observed that, by tuning defocusing parameter, it is possible to optimize the illumination uniformity and throughput being offered to densely deployed IoT devices in a room. However, more research is needed to further optimize the system and consider other parameters beyond the defocus amount, such as the separation of LEDs on the LED array and LEDs' transmit powers. Successful implementation of multi-datastream VLC networks depends mostly on the delicate balancing of illumination uniformity with the bare-minimum needed SINR for reliable detection of bit streams. This balancing also requires future research on how to best associate mobile receivers in the room to specific LEDs on the bulb. In solving this association problem, flexibility of the controller circuitry driving the LED array will have to be considered as part of the design. In our approach, we have assumed that only one mobile receiver is assigned to an LED on the array. It is possible to consider multiple receiver per LED and multiple LEDs per receiver. Developing heuristics for these cases will increase the potential benefit of the dome bulb in multi-datastream VLC networks.

ACKNOWLEDGMENTS

This work was supported in part by U.S. National Science Foundation award 1836741.

REFERENCES

[1] H. Ando and S. Ryu, "Simultaneous Dual Data Stream Transmission Using RGB and Phosphor-based White LEDs," in *Proceedings of IEEE Asia Communications and Photonics Conference (ACP)*, pp. 1-3, 2018.

[2] Y. Wang, Y. Wang, N. Chi, J. Yu, and H. Shang, "Demonstration of 575-Mb/s downlink and 225-Mb/s uplink bi-directional SCM-WDM visible light communication using RGB LED and phosphor-based LED," *Optics Express,* vol. 21, no. 1, pp. 1203-1208, 2013.

[3] S. I. Mushfique, A. Alsharoa, and M. Yuksel, "Optimization of SINR and Illumination Uniformity in Multi-LED Multi-Datastream VLC Networks," *IEEE Transactions on Cognitive Communications and Networking,* 2020. DOI: 10.1109/TCCN.2020.2972310

[4] H. Alshaer and H. Haas, "Bidirectional LiFi attocell access point slicing scheme," *IEEE Tran. on Network & Service Management,* vol. 15, no. 3, pp. 909-922, 2018.

[5] S. Cincotta, C. He, A. Neild, and J. Armstrong, "Indoor visible light positioning: Overcoming the practical limitations of the quadrant angular diversity aperture receiver (QADA) by using the two-stage QADA-plus receiver," *Sensors,* vol. 19, no. 4, p. 956, 2019.

[6] P. Nabavi and M. Yuksel, "Conformal VLC Receivers with Photodetector Arrays: Design, Analysis and Prototype," in *Proceedings of IEEE International Conference on Communications (ICC)*, pp. 1-7, 2019.

[7] H. Haas, L. Yin, C. Chen, S. Videv, D. Parol, E. Poves, H. Alshaer, and M. S. Islim, "Introduction to indoor networking concepts and challenges in LiFi," *J. of Optical Communications & Networking,* vol. 12, no. 2, pp. A190-A203, 2020.

[8] S. Saghaye Polkoo and C. K. Renshaw, "Imaging-based beam steering for free-space optical communication," *Applied Optics,* vol. 58, no. 13, pp. D12-D21.

[9] A. M. Vegni and M. Biagi, "Optimal LED placement in indoor VLC networks," *Optics Express*, vol. 27, pp. 8504-8519, 2019.

[10] M. Obeed, A. M. Salhab, M. Alouini, and S. A. Zummo, "On Optimizing VLC Networks for Downlink Multi-User Transmission: A Survey," *IEEE Communications Surveys & Tutorials*, vol. 21, no. 3, pp. 2947-2976, 2019.

[11] T. V. Pham and A. T. Pham, "Coordination/Cooperation Strategies and Optimal Zero-Forcing Precoding Design for Multi-User Multi-Cell VLC Networks," *IEEE Tran. on Communications*, vol. 67, no. 6, pp. 4240-4251, June 2019.

[12] J. Wang, C. Jiang, H. Zhang, X. Zhang, V. C. M. Leung and L. Hanzo, "Learning-Aided Network Association for Hybrid Indoor LiFi-WiFi Systems," *IEEE Transactions on Vehicular Technology*, vol. 67, no. 4, pp. 3561-3574, April 2018. DOI: 10.1109/TVT.2017.2778345.

[13] R. Zhang, J. Wang, Z. Wang, Z. Xu, C. Zhao and L. Hanzo, "Visible light communications in heterogeneous networks: Paving the way for user-centric design," *IEEE Wireless Communications*, vol. 22, no. 2, pp. 8-16, April 2015.

[14] S. Shao and A. Khreishah, "Delay Analysis of Unsaturated Heterogeneous Omnidirectional-Directional Small Cell Wireless Networks: The Case of RF-VLC Coexistence," *IEEE Transactions on Wireless Communications*, vol. 15, no. 12, pp. 8406-8421, December 2016. DOI: 10.1109/TWC.2016.2614822.